Wind and Structures, *Vol. 25, No. 3 (2017) 283-299*
DOI: https:// doi.org/10.12989/was.2017.25.3.283

Aerodynamic admittances of bridge deck sections: Issues and wind field dependence

Zhitian Zhang*[1,2], Weifeng Zhang[1,2a] and Yaojun Ge[3b]

[1]*Wind Engineering Research Center, School of Civil Engineering, Hunan University, Changsha 410082, China*
[2]*Hunan Provincial Key Laboratory of Wind and Bridge Engineering, China*
[3]*State Key Laboratory of Disaster Reduction in Civil Engineering, Tongji University, ShangHai, China*

(Received January 19, 2017, Revised August 2, 2017, Accepted August 12, 2017)

Abstract. Two types of aerodynamic admittance function (AAF) that have been adopted in bridge aerodynamics are addressed. The first type is based on a group of supposed relations between flutter derivatives and AAFs. In so doing, the aero-elastic properties of a section could be used to determine AAFs. It is found that the supposed relations hold only for cases when the gust frequencies are within a very low range. Predominant frequencies of long-span bridges are, however, far away from this range. In this sense, the AAFs determined this way are of little practical significance. Another type of AAFs is based on the relation between the Theodorsen circulation function and the Sears function, which holds for thin airfoil theories. It is found, however, that an obvious illogicality exists in this methodology either. In this article, a viewpoint is put forward that AAFs of bluff bridge deck sections are inherently dependent on oncoming turbulent properties. This kind of dependence is investigated with a thin plate and a double-girder bluff section via computational fluid dynamics method. Two types of wind fluctuations are used for identification of AAFs. One is turbulent wind flow while the other is harmonic. The numerical results indicate that AAFs of the thin plate agree well with the Sears AAF, and show no obvious dependence on the oncoming wind fields. In contrast, for the case of bluff double-girder section, AAFs identified from the turbulent and harmonic flows of different amplitudes differ among each other, exhibiting obvious dependence on the oncoming wind field properties.

Keywords: bridge; bluff; aerodynamic admittance; wind field; flutter derivative

1. Introduction

Buffeting of long-span bridges due to wind fluctuations have not been able to be evaluated accurately. Difficulties arise from many aspects, among which the most challenging one is the so-called aerodynamic admittance function (AAF). An AAF links the aerodynamic loads developed on a section, such as aerodynamic lift, drag, or torque, to the oncoming wind turbulences. Traditionally, an AAF for a given section is considered a function of the reduced frequency only, independent on turbulence properties, such as turbulence intensity, power spectrum density, etc.

The concept of AAF originates from the issue of unsteady aerodynamic loads developed on a

*Corresponding author, Professor, E-mail: zhangzhitian@hnu.edu.cn
[a] Ph.D. candidate, Email: 286502694@qq.com
[b] Professor, Email: yaojunge@tongji.edu.cn

Copyright © 2017 Techno-Press, Ltd.
http://www.techno-press.org/?journal=was&subpage=7 ISSN: 1226-6116 (Print), 1598-6225 (Online)

thin airfoil due to approaching wind fluctuations. Von Karman and Sears (1938) first determined the aerodynamic lift and torque on a thin airfoil due to a general expression of wind velocity, distributed along the chord. Then, Sears (1941) specified this achievement to the case of a vertical, sinusoidal approaching gust, by assuming the vertical wind velocity $w(x)$ is equivalent to relative sinusoidal sectional velocity. Liepmann (1952) simplified Sears's formulation and applied it to airfoil buffeting analysis. Later, Davenport (1962a, b) adopted Sears's function to describe the aerodynamic lift developed on the deck of a truss girder suspension bridge, and referred to it as an aerodynamic admittance function. From then on, AAFs of the same nature as that for thin airfoil sections, namely independent on the oncoming turbulence, have been practiced extensively in bridge aerodynamics (Ge and Zhao 2014, Zhang and Ge 2011, Han *et al*. 2010, Ge *et al*. 2009, Zhu *et al*. 2003, etc.). Exhaustive citations of this kind of applications are not presented here due to space limitation. However, from time to time, evidences from published literature show that AAFs display dependence on the wind properties. Among them, Larose and Mann (1998) investigated sections of different aspect ratios, and the results indicated AAFs differs significantly among different types of turbulent wind fields; Matsuda *et al.* (1999) pointed out that aerodynamic admittance depended on types of wind tunnel flow; Rasmussen *et al*. (2010) calculated AAFs of sectional models by using discrete vortex method, and the results showed even the AAFs of a flat plate exhibited wind field dependence to some extent; More recently, Zhu and Xu (2014) performed sectional model tests of a bridge deck, and the results indicated that AAFs are very different among different wind fields. Notwithstanding these reported findings, essential properties of AAFs of bluff bridge sections, including uniqueness and dependence on oncoming wind fields, have not yet been addressed.

In this work, issues arise from typical AAF models in bridge aerodynamics are firstly addressed. These models are determined uniquely by reduced frequency and independent on the wind field, as is characteristic of to thin airfoil theories. Then, uniqueness of AAFs of a typical bluff section is investigated via computational fluid dynamics. Although wind fields in nature are always 3-dimensional, the AAFs addressed here are still 2-dimensional, and the effects arise from span-wise direction are able to be merged into spatial coherence.

2 Issues in existing AAF models

As bluff deck sections are concerned, motions-induced aerodynamic loads, or aeroelastic effects, can be expressed in terms of flutter derivatives (Scanlan 1971). Usually, the flutter derivatives are able to be obtained experimentally. This methodology has been developed, employed extensively over the years. With the reliability of flutter derivatives, Scanlan (1999, 2000) tried to establish a relation between motion-induced aeroelastic effects and wind turbulence induced aerodynamic effects. In his work, a form of AAF is obtained via flutter derivatives. For example

$$|\chi_{L'}|^2 = K^2\left[(H_1^*)^2 + (H_4^*)^2\right]/(C_L')^2 \tag{1}$$

where $\chi_{L'}$ is complex aerodynamic lift admittance function; $K = B\omega/U$ is reduced frequency; B is reference width; ω is circular frequency; U is mean wind velocity; H_1^*, H_4^* are flutter derivatives; $C_L' = dC_L/d\alpha$ is the derivative of aerostatic lift coefficient C_L with respect to wind angle of attack α.

The whole set of AAFs, associated with aerodynamic torque or lift resulted from vertical and horizontal turbulent components, are able to be related to flutter derivatives. This method has been broadly employed (Caracoglia and Jones 2003, Caracoglia 2008, Chen and Matsumoto 2000, Chen and Kareem 2001, Tubino 2005, etc.). Buffeting loads can be expressed in this way by flutter derivatives. For example, the auto-PSD of the lift may be denoted as

$$S_{LL}(K) = \left(\frac{1}{2}\rho UBC_L'\right)^2 \cdot |\chi_{L'}|^2 \cdot S_{ww} \tag{2}$$

where S_{ww} is auto-PSD of the vertical gust.

The crux of this method is the assumption that leads to those relations; that is, wind gusts are supposed to equal to or approximate those of the section's relative rigid motions. However, except for the extreme case that the gust frequency being infinitely low, there is no equivalence between a wind gust, which varies in both space and time, and a rigid motion, which varies only in time. According to Sears (1941), a vertical wind gust, $w = e^{\mathrm{i}\omega t}e^{-\mathrm{i}\omega x/U}$, is able to be expanded to

$$w = e^{\mathrm{i}\omega t}\left\{J_0(k) + 2\sum_{n=1}^{\infty}(-\mathrm{i})^n J_n(k)\cos n\theta\right\} = C_{const}e^{-\mathrm{i}\omega t} + 2e^{\mathrm{i}\omega t}\sum_{n=1}^{\infty}(-\mathrm{i})^n J_n(k)\cos n\theta \tag{3}$$

where $k = b\omega/U = 0.5K$; θ is a coordinate, for a section of chord length of 2 (physical coordinate x from -1 to 1), cos θ = -1 at the leading edge and cos θ = 1 at the trailing edge; In between, the relationship between x and θ is x = cos θ.

The first four terms in eq.3 are plotted in Fig. 1, where the results are calculated by using Eq. (3).

It is noticed that only the first and second terms bear resemblance to rigid motions, corresponding respectively to a vertical motion $\dot{h} = e^{-\mathrm{i}\omega t}$ and a torsional motion $\dot{\alpha} = e^{-\mathrm{i}\omega t}$. Other higher-order terms have no equivalence to rigid motions, and, actually, they bear resemblance to the chord's flexible deformations. It is neglecting of these higher-order velocity patterns that lead to the relations between flutter derivatives and AAFs.

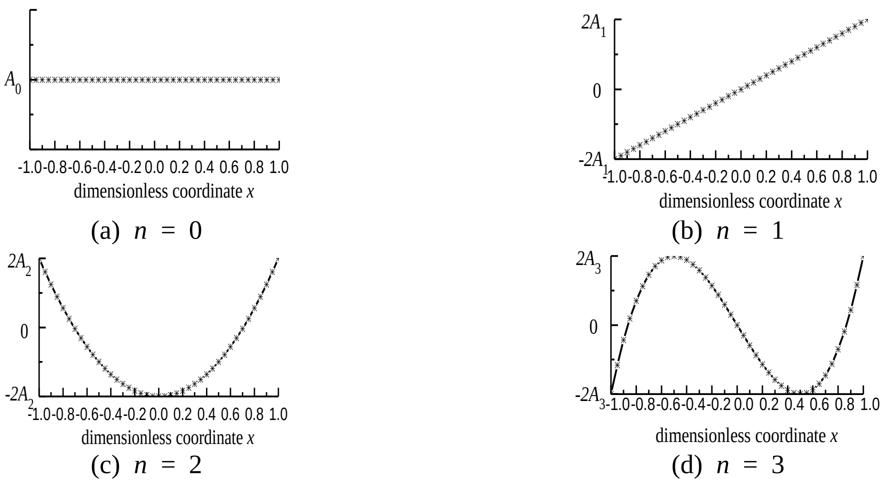

Fig. 1 Basic vertical velocity distributions of the first four terms in Eq. (3)

The most direct consequence of this approach would be wrong limiting characteristics. Take a thin plate section for example, of which both the flutter derivatives and the AAF (Sears function) are known, and the AAF calculated from flutter derivatives can be compared with the known Sears function. The comparison is shown in Fig. 2. It is noticed the Sears function approaches 0 as K approaches infinite. However, the AAF from flutter derivatives approaches a non-zero value 0.25. A nonzero limit of an AAF is physically incorrect since the lift due to a gust with infinite small wave length should always converge to zero. In essence, this incorrectness can be ascribed to the assumption of equivalence between Küssner function and Wagner's indicial function, which actually doesn't hold in both streamlined and bluff sections (Zhang *et al.* 2013).

When bluff sections are concerned, limit values of the AAFs so obtained can be arbitrary, depending on specific flutter derivatives identified.

It is also noticed that, when K is very small, the flutter-derivatives-based AAF approaches asymptotically to Sears AAF; therefore, this method is applicable to a certain range of reduced frequency. However, predominant buffeting frequencies of long-span bridges are quite out of this range, as seem in Fig. 3, where examples include the Third Nanjin Bridge (Zhu *et al.* 2007), the Hardanger Bridge (Øiseth *et al.* 2011), the Second Severn Bridge (Macdonald *et al*. 2003), the Tsing Ma Bridge (Xu e*t al*. 2000), the East Coast Sea Bridge (Zhang *et al*. 2005), and the Akashi-Kaikyo Bridge (Minh *et al.* 1999). The reduced frequencies (deck vertical) shown in Fig. 3 cover a wind velocity range from 10 to 30 m/s. Referring to Fig. 2, it is noticed that for these cases, K locates somewhere in the vicinity of (or between) 1 to 10; therefore, evaluating AAF by this method could result in substantial deviations.

To remedy nonzero limit values resulted from this method, a quasi-steady method based on spatial coherence of turbulence has to be introduced (Scanlan 2000, 2001), as

$$|\chi_{L'}|^2 = \frac{K^2}{(C_L')^2}\left[\left(H_1^*\right)^2 + \left(H_4^*\right)^2\right]\cdot R(c), \tag{4}$$

where

$$R(c) = \int_0^B\int_0^B \exp\left[-c_0\frac{\sigma_w}{U}n|x_1 - x_2|\right]dx_1 dx_2 \tag{5}$$

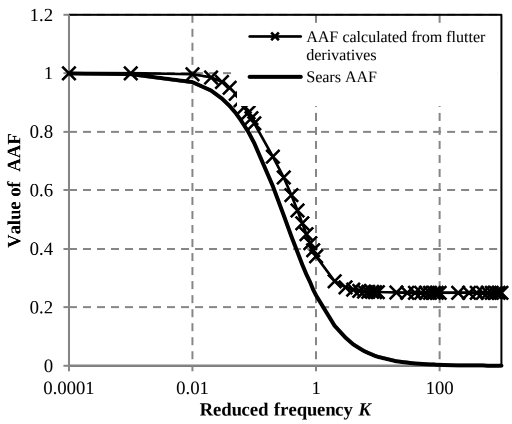

Fig. 2 AAFs of Sears and calculated from flutter derivatives

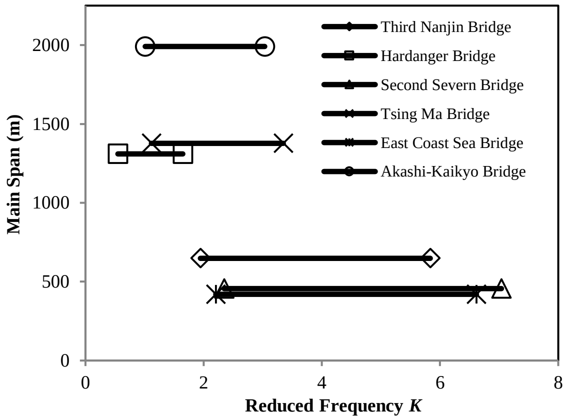

Fig. 3 Range of K of some typical bridges from U = 10 to 30 m/s

is an coefficient determined by the along-wind coherence of vertical gusting over the whole chord width; c_0 a constant reflecting the level of coherence, σ_w/U the turbulence intensity and n the frequency of turbulent component. Note that in this situation $R(c) \to 0$ when $n \to \infty$ (or $K \to \infty$).

A number of researchers have tried to determine AA functions basing on another point of view of "equivalent" Theodorsen function (Hatanaka and Tanaka 2002, 2008, Costa 2007, Costa *et al.* 2007).

The idea of this method is, firstly, supposing a known relation between Theodorsen circulation function $C(k)$ and Sears function $\chi_s(k)$, namely

$$\chi_s(k) = [J_0(k) - iJ_1(k)]C(k) + \mathrm{i}J_1(k) \tag{6}$$

is applicable to bluff deck sections, where k = 0.5K. Note $J_0(k)$ and $J_1(k)$ in Eq. (6) are Bessel functions. Then, according to relations between flutter derivatives and indicial functions (Scanlan 2000), one could obtain equivalent indicial functions from known flutter derivatives, for example

$$4k(H_1^* - \mathrm{i}H_4^*) = C_L' \, [\varphi_{Lh}(0) + \overline{\varphi}_{Lh}'] \tag{7}$$

where φ_{Lh} is an indicial function describing evolution of the aerodynamic lift due to vertical motion, $\overline{\varphi}_{Lh}'$ is Fourier transform of the derivative of φ_{Lh} with respect to dimensionless time $s = Ut/b$. Once equivalent indicial functions are obtained, an "equivalent" Theodorsen function, $C_{eq}(k)$, can be determined by Garrick's interrelation $C(k) = \varphi(0) + \overline{\varphi}'$ (Garrick 1938). Finally, an "equivalent" Sears admittance function can be written according to (6), as

$$\chi_{eq,s}(k) = [J_0(k) - \mathrm{i}J_1(k)]C_{eq}(k) + \mathrm{i}J_1(k) \tag{8}$$

The process of acquiring AAFs according to equivalent Theodorsen functions is shown in Fig. 4. An issue of logicality arises from this methodology. According to Theodorsen's work (Theodorsen 1935), $C(k)$ is expressed as

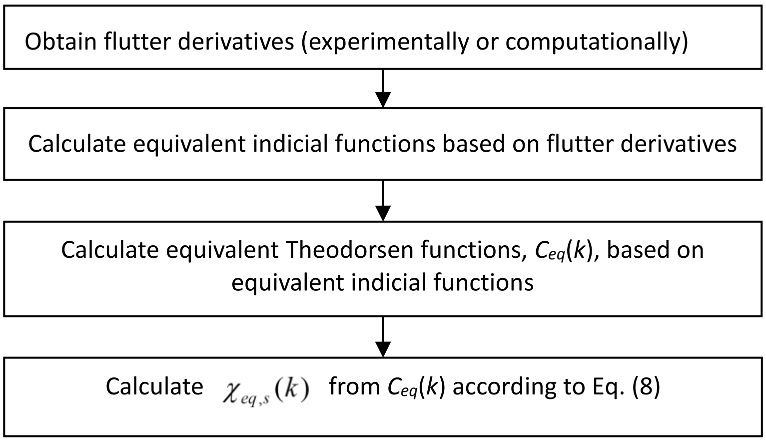

Fig. 4 The process of acquiring AAFs according to equivalent Theodorsen functions

$$C(k) = F + \mathrm{i}G = \frac{-J_1(k) + \mathrm{i}Y_1(k)}{-[J_1(k) + Y_0(k)] + \mathrm{i}[Y_1(k) - J_0(k)]} \tag{9}$$

where the Bessel functions, J_0, J_1 , Y_0 and Y_1, are given as follow

$$J_0(k) = \frac{2}{\pi}\int_1^\infty \frac{\sin kx}{\sqrt{x^2-1}}dx \, , \quad J_1(k) = -\frac{2}{\pi}\int_1^\infty \frac{x\cos kx}{\sqrt{x^2-1}}dx \, , \quad Y_0(k) = -\frac{2}{\pi}\int_1^\infty \frac{\cos kx}{\sqrt{x^2-1}}dx \, , \quad Y_1(k) = -\frac{2}{\pi}\int_1^\infty \frac{x\sin kx}{\sqrt{x^2-1}}dx \tag{10}$$

Obviously, these functions are not only combinations between $C(k)$ and $\chi_s(k)$, as shown by Eq. 6, but also they are components of both $C(k)$ and $\chi_s(k)$. Thus, if an "equivalent" form of $C_{eq}(k)$ is used to replace $C(k)$, there is no justification for J_0 and J_1 to remain their original forms unchanged, since the two functions themselves are parts of $C(k)$. However, on the other hand, 'equivalent' forms of J_{0eq} and J_{1eq} are always unavailable.

An important property of the AAF of a thin airfoil section, $\chi_s(k)$, is its independence on the oncoming wind fluctuations. Scrutiny on the derivation of $\chi_s(k)$ reveals the following prerequisites that lead to this kind of independence (von Karman and Sears 1938, Sears 1941): (i) The aerodynamic performances of a section can be determined by its body midline, and influences of the thickness along the midline are negligible; (ii) The vertical motion and/or the wind fluctuation at any location is small, so that the trail of vortices formed behind the section lie straightly upon the X-axis; (iii)The theory of complex potential of incompressible inviscid flow is applicable to the whole field around the section, Therefore, induced circulations around the section from vortices located behind can be integrated along the X-axis from 1 to ∞, based on the principle of superposition.

None of the above prerequisites is fulfilled in cases of bluff body sections, where the mean and turbulent wind structures developed around and behind the body depend on the oncoming turbulence structures; body thickness or body shapes are of primary importance to the formation of the flow field around; wind fluctuations could be no longer small compared to the mean wind speed; theory of potential flow is inapplicable and severe detached flow could be involved. In such a situation, it is logic to reason that AAFs depend on the oncoming turbulent field. Verification of this basic property is of significance in engineering, since it determines the methodology used to obtain AAFs.

In the following sections, this basic property is investigated by means of CFD, with a bluff section and a thin plate section concerned.

3. Wind-field dependence of AAFs

3.1 Computational set-up

Two typical sections are considered in comparison to investigate the dependence of AAFs on oncoming turbulent flows. One is a very streamlined plate with a very high width-to-height aspect ratio, and the other is a bluff double-girder section common to bridge decks. The two sections have almost the same width of 310 mm, as shown in Fig. 5. The thickness of the flat plate is 3 mm, and the height of the double-girder section is 33 mm.

Fig. 6 shows the computational domain. The synthesis method by Davidson (2005) is employed in this study for the inlet flow set up. The adopted method generates a divergence-free fluctuating velocity filed that satisfies the von Karman's wind spectrum. A pressure-outlet condition is used at the outlet, of which one advantage is that the backflow can be considered during the simulation.

In cases when sinusoidal wind fluctuations are used, the vertical wind component across the whole inlet is given as

$$w = A\sin(\omega t) \tag{11}$$

where A is velocity amplitude and ω is circular frequency. Simultaneously, a vertical wind component

$$w(x,t) = A\sin[\omega(t - x/U)] \tag{12}$$

is given along both the top and bottom boundaries, as shown in Fig. 6. At section surfaces, no-slip conditions are imposed.

Computations have been conducted using commercial software ANSYS Fluent. The flow field is spatially discretized into multi-block structured grids. The gridding applied to the sections are shown in Fig. 7, and the number of the grids around the flat plate and the double-girder are respectively 312,000 and 384,000. Progressing in time is accomplished by a second order fully implicit scheme. Time steps used in simulations is set to $\Delta t = 0.0026B/U$, which ensures Courant number of less than 1 for almost all the computational domain except a few cells at the end of the section. The simulations have been performed with time duration T_a=1100.4B/U = 42.32 s in order to result in a long enough sample.

RANS method is adopted, of which a large number of branches have been developed to simulate the turbulence viscosity. In this study, the SST k-ω method is used for turbulence modeling, which uses turbulent kinetic energy k and turbulence frequency ω to describe turbulence viscosity. The transport equations of these two variables are given as follow

$$\frac{\partial}{\partial t}(\rho k) + \frac{\partial}{\partial x_i}(\rho k u_i) = \frac{\partial}{\partial x_j}\left((\mu + \frac{\mu_t}{\sigma_k})\frac{\partial k}{\partial x_j} \right) + G_k - Y_k \tag{13}$$

$$\frac{\partial}{\partial t}(\rho\omega)+\frac{\partial}{\partial x_i}(\rho\omega u_i)=\frac{\partial}{\partial x_j}\left((\mu+\frac{\mu_t}{\sigma_w})\frac{\partial\omega}{\partial x_j}\right)+G_\omega-Y_\omega+D_\omega \tag{14}$$

where k is turbulence kinetic energy; turbulence frequency $\omega = \varepsilon/k$; ε is turbulence dissipation; G_k production of k; G_ω is production of ω; Y_k is the dissipation of k; Y_ω is the dissipation of ω; D_ω is cross diffusion term;

The turbulent Prantdl number σ_k and σ_ω are computed according to

$$\sigma_k=\frac{1}{F_1/\sigma_{k,1}+(1-F_1)/\sigma_{k,2}} \tag{15}$$

and

$$\sigma_w=\frac{1}{F_1/\sigma_{\omega,1}+(1-F_1)/\sigma_{\omega,2}} \tag{16}$$

where

$$F_1=\tanh(\Phi_1{}^4) \tag{17}$$

and

$$\Phi_1=\min\left[\max\left(\frac{\sqrt{k}}{0.09\omega y},\frac{500\mu}{\rho y^2\omega}\right),\frac{4\rho k}{\sigma_{w,2}D_w{}^+y^2}\right] \tag{18}$$

$$D_W{}^+=\max\left[2\rho\frac{1}{\sigma_{\omega,2}}\frac{1}{\omega}\frac{\partial k}{\partial x_j}\frac{\partial\omega}{\partial x_j},10^{-10}\right] \tag{19}$$

$$F_2=\tanh(\Phi_2{}^2) \tag{20}$$

and

$$\Phi_2=\max\left[2\frac{\sqrt{k}}{0.09\omega y},\frac{500\mu}{\rho y^2\omega}\right] \tag{21}$$

Finally, with k and ω resolved by Eqs. (13) and (14), the turbulent viscosity μ_t is determined by

$$\mu_t=\frac{\rho k}{\omega}\frac{1}{\max\left[1,\frac{SF_2}{a_1\omega}\right]} \tag{22}$$

where $S=\sqrt{S_{ij}S_{ij}}$, and S_{ij} is the rate-of-strain tensor.

Constants involved in the model are given as: $\sigma_{k,1}=1.176$, $\sigma_{\omega,1}=2.0$, $\sigma_{k,2}=1.0$, $\sigma_{\omega,2}=1.168$, $a_1=0.31$, $\beta_{i,1}=0.075$, $\beta_{i,2}=0.0828$, $\alpha_{\infty}=0.52$, $\alpha_0=1/9$, $R_{\omega}=2.95$, $\beta_{\infty}^{*}=0.52$.

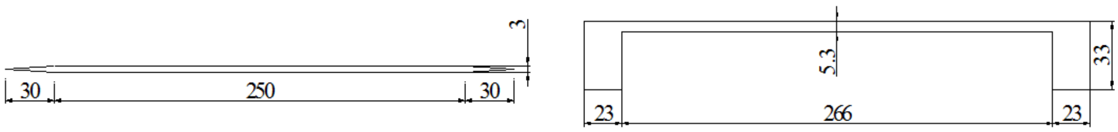

(a) Thin plate section (b) Double-girder section

Fig. 5 Sections used for CFD (unit: mm)

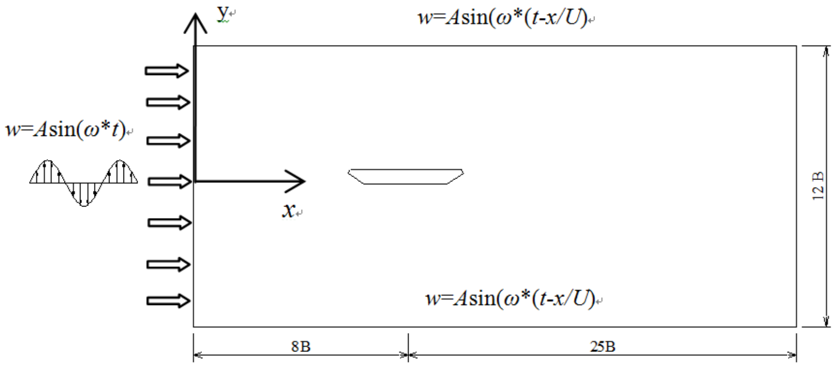

Fig. 6 Domain and boundary condition for CFD, where B is section width

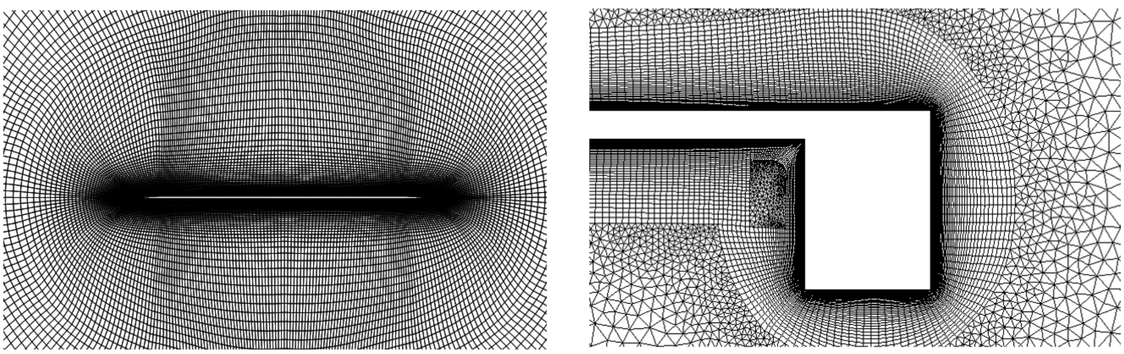

(a) Thin plate section (b) Double-girder section

Fig. 7 Meshing around the models

3.2 Identification of AAFs

When only vertical wind component is involved, as considered in the numerical example in this study, the aerodynamic lift and torque are given as

$$L_b(t) = \rho UB\left(\frac{1}{2}(C_L'(\alpha) + C_D(\alpha))\chi_{Lw}w(t)\right) \tag{23}$$

$$M_b(t) = \rho UB^2\left(\frac{1}{2}C_M'(\alpha)\chi_{Mw}w(t)\right) \tag{24}$$

where $L_b(t)$ and $M_b(t)$ are buffeting lift and torque respectively; $C_D(\alpha)$, $C_L(\alpha)$, $C_M(\alpha)$ are aerostatic drag, lift, and torque coefficients, functions of wind angle of attack α; $C_L'(\alpha)$, $C_M'(\alpha)$ are derivatives of $C_L(\alpha)$ and $C_M(\alpha)$ with respect to α; χ_{Lw}, χ_{Mw} are complex AAFs dependent on reduced frequency.

Taking Fourier transforms of Eqs (23) and (24) obtains frequency spectrum of the lift and torque, as

$$S_L = (\frac{1}{2}\rho UB)^2(C_L' + C_D)^2\left|\chi_{Lw}\right|^2 S_w \tag{25}$$

$$S_M = (\frac{1}{2}\rho U^2 B)^2 C_M'^2\left|\chi_{Mw}\right|^2 S_w \tag{26}$$

where S_L, S_M, S_w are frequency spectra of the lift, torque, and vertical wind fluctuation, respectively. According to Eqs (25) and (26), the square of modules of AAFs can be denoted by

$$\left|\chi_{Lw}\right|^2 = \frac{S_L}{(\frac{1}{2}\rho UB)^2(C_L' + C_D)^2 S_w} \tag{27}$$

$$\left|\chi_{Mw}\right|^2 = \frac{S_M}{(\frac{1}{2}\rho U^2 B)^2 C_M'^2 S_w} \tag{28}$$

For comparison in the subsequent text, the square of module of Sears AAF is also given here by the Liepmann approximation, as

$$\left|\chi_L(k)\right|^2 = \frac{1}{1+2\pi^2 k} \tag{29}$$

3.3 Turbulence generating

Two kind of wind fields are simulated in this study for identification of AAFs. The first one is turbulent wind field, and the turbulence at the inlet is simulated using the method put forward by

Davison *et al.* (2005), which generates turbulent wind histories for given turbulence intensity, integral length, or power spectrum density. The von Karman wind spectrum is adopted in this work. Fig. 8 shows the targeted spectrum and simulated spectrum at the leading edge of the section in the computational field. It is found that the simulated agrees quite well with the targeted wind spectrum.

Another kind of wind field is vertical wind fluctuation with a single frequency. It is generated by forced inlet and boundary conditions (Tang *et al.* 2015), as introduced in section 3.1. As shown in Fig. 9, this method generates extremely pure harmonic wind fluctuations. By changing the frequency of the harmonic wind fluctuations, the desired range of frequency can be covered discretely.

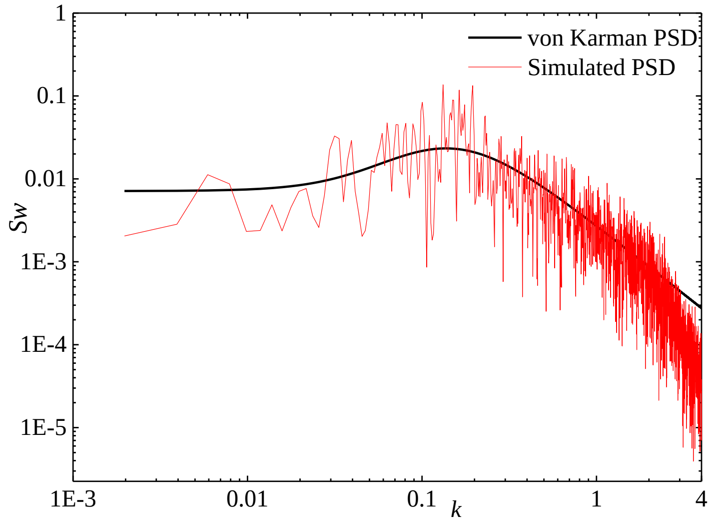

Fig. 8 Wind spectra of the vertical gust at (x, y) = (5B, 0)

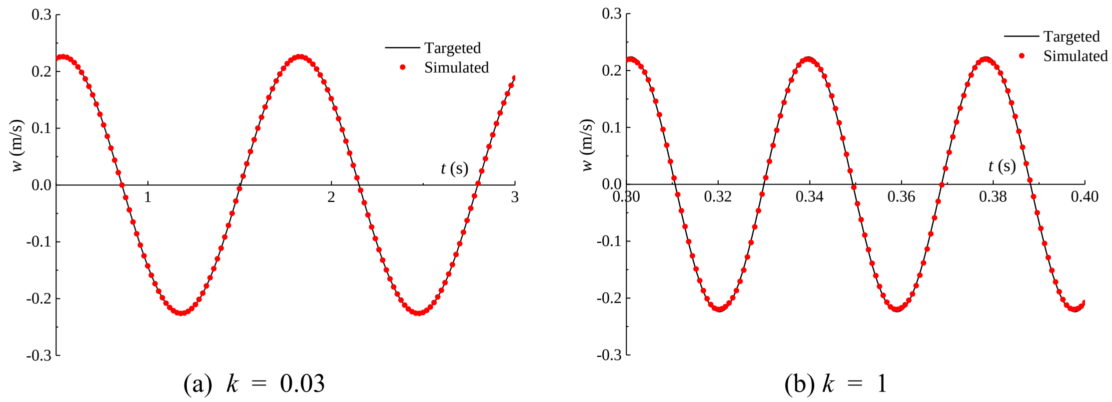

Fig.9 Vertical sinusoidal gusts obtained at the leading edge (x , y) = (5B , 0)

3.4 Results and discussion

Fig. 10 presents the squares of module of AAFs obtained from the above mentioned two types of wind field. Corresponding PSD of the turbulence (Wind field 1 in Table 1) at the leading edge is shown in Fig. 8. For the harmonic wind field, the amplitude of wind velocity at all frequencies is 0.226 m/s. The mean wind speed and turbulence intensity of both wind fields are 8 m/s and 2%, respectively. It is noticed that, for the case of flat plate, computed AAF in sinusoidal wind field is in very good agreement with the sears function, and this verifies to some extent the reliability of the employed CFD model and algorithm. For the case of double-girder section, there is significant difference between computed AAF and Sears AAF. This is expected results since double-girder section is of obvious bluff body properties. On the other hand, obvious disagreement is found between AAFs from turbulent and harmonic wind fields in the frequency range where signature turbulence occurs, and this contributes to the property of wind field dependence of AAFs of bluff bodies.

If an AAF is independent on oncoming wind fields, it can be reflected in many aspects: (i) First of all, its value at frequency ω_i, $\chi(\omega_i)$, is independent on the frequency spectrum or PSD of the wind $S_w(\omega_i)$; (ii)Further, $\chi(\omega_i)$ is independent on the PSD of the wind at any other frequency $\omega_j \neq \omega_i$, say $S_w(\omega_j)$. All these properties are necessary conditions of an AAF being independent on oncoming wind field, and can be used to examine this kind of independence.

In what follows, we examine the dependence of $\chi(\omega_i)$ on $S_w(\omega_i)$, and the change of $S_w(\omega_i)$ can be realized simply by changing amplitude of the harmonic wind fluctuation, since $S_w(\omega_i)$ is the square of the module of the frequency spectrum of $w(t)$ at ω_i. To this end, both the flat plate and double-girder sections are investigated. By changing the frequency of a harmonic wind field, the aerodynamic loads developed on the sections are calculated, according to which the AAFs at different frequencies are able to be identified.

Three levels of vertical wind velocity are used, as shown in Table 1, varying from 0.22 m/s to 1.333 m/s. Typical time histories of lift developed on the thin plate and on the double-girder section are plotted in Figs. 11 and 12, respectively. It is noticed that, in the case of double-girder section, aerodynamic lift is periodic (see Fig. 12(a)), even in uniform flow, indicating regular vortex shedding.

Figs. 13 and 14 plot respectively $\left|\chi_{Lw}\right|^2$ and $\left|\chi_{Mw}\right|^2$ versus reduced frequency k. It is found that the identified AAFs of the thin plate section exhibit independence on the amplitude of the wind fluctuation, or, at best, exhibit very weakly dependence on it, and this weak dependence can be within numerical uncertainties. On the other hand, in the case of the double-girder section which possesses typical bluff body properties, there is obvious dependence of $\left|\chi_{Lw}\right|^2$ and $\left|\chi_{Mw}\right|^2$ on the amplitude of the wind fluctuation, especially in the higher frequency range where signature turbulence interact significantly with the oncoming wind fluctuations.

Referring to Eq. (23), if χ_{Lw} is uniquely determined by the reduced frequency K (or k), then, for a given reduced frequency K, the ratio of the amplitude of lift to that of the wind fluctuation would be a constant, independent on the oncoming wind field, as

$$\frac{\left|L_b(t)\right|}{\left|w(t)\right|} = \left|\rho UB\left(\frac{1}{2}(C_L'(\alpha) + C_D(\alpha))\chi_{Lw}\right)\right| = const\,. \tag{30}$$

That means, for a sinusoidal input wind fluctuation

$$w(t) = A_0 \sin(\omega t) \tag{31}$$

and the output aerodynamic lift fluctuation

$$L_b(t) = A_1 \sin(\omega t + \phi) \tag{32}$$

the ratio of A_1/A_0 would be a constant that is independent on A_0. This property is checked at reduced frequency $K = 0.8$, as shown in Fig. 15. It is noticed while the ratios in the case of flat plate varies only very slightly, those in the case of double-girder section varies drastically among different wind fields, indicating a significant dependence on the oncoming wind property.

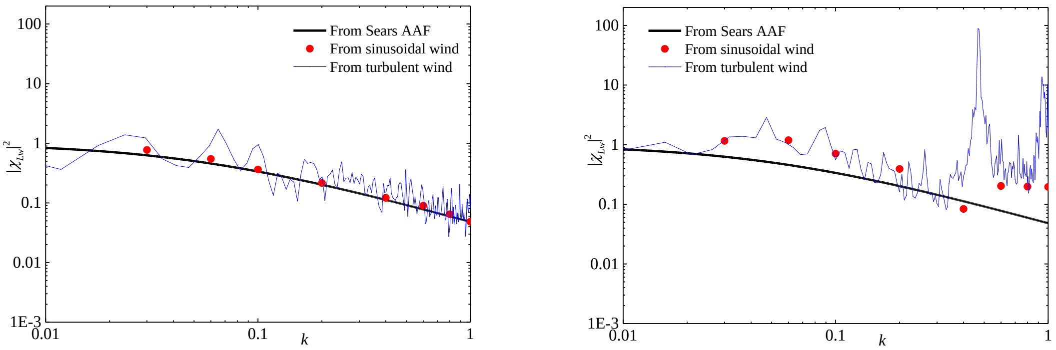

(a) Flat plate section (b) Double-girder section

Fig. 10 Aerodynamic lift admittances under two types of wind fields

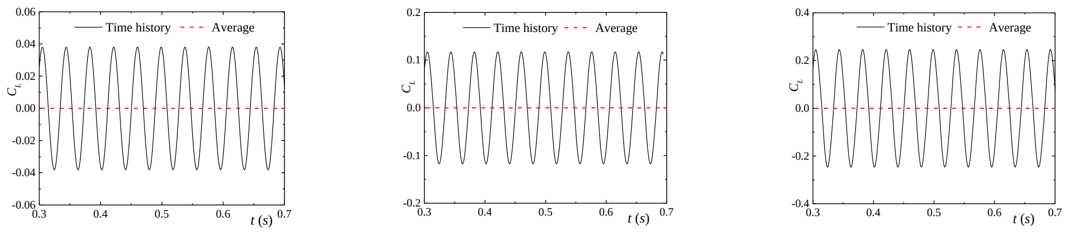

(a) wind field 1 (b) wind field 2 (c) wind field 3

Fig. 11 Time histories of lift coefficients for the plate section ($k = 0.8$)

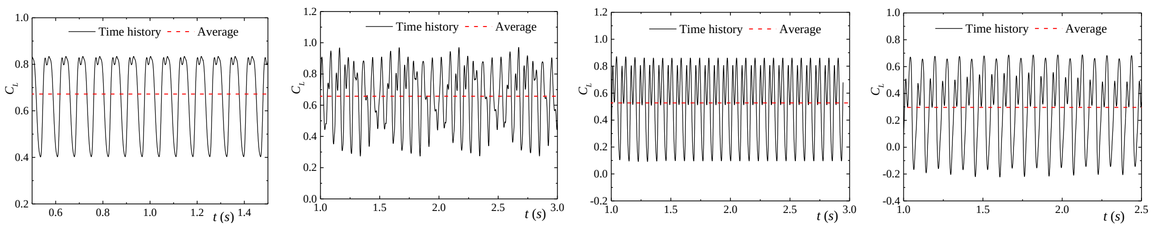

(a) uniform flow (b) wind field 1 (c) wind field 2 (d) wind field 3

Fig. 12 Time histories of lift coefficients for the double-girder section ($k = 0.8$)

Table 1 Velocity amplitudes (k = 0.8)

	wind filed 1	wind field 2	wind field 3
Velocity amplitude A_0 (m/s)	0.220	0.664	1.333
Equivalent turbulence intensity	2%	6%	12%

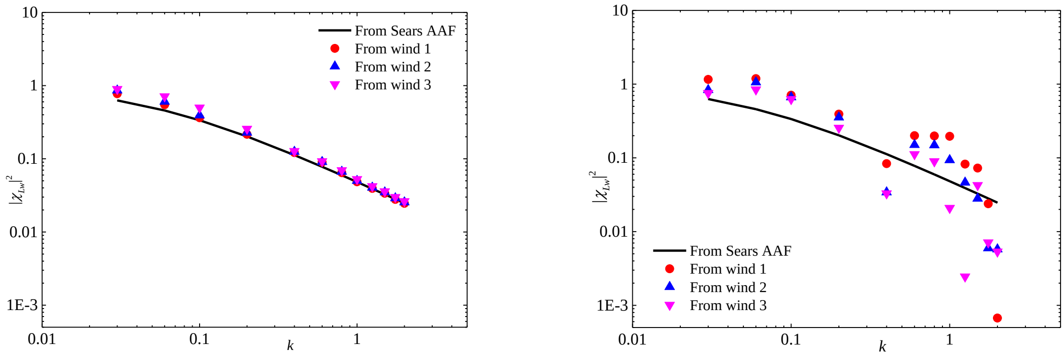

(a) thin plate (b) double-girder section

Fig. 13 Admittance function $\left|\chi_{Lw}\right|^2$

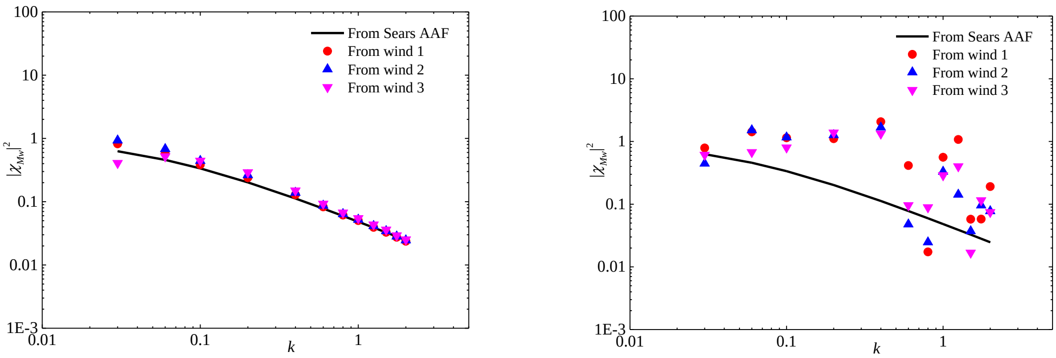

(a) thin plate (b) double-girder section

Fig. 14 Admittance function $\left|\chi_{Mw}\right|^2$

A number of researchers identified AAFs of bridge deck sections in wind tunnels (Larose *el al.* 1998, Larose and Mann 1998, Diana *el al.* 2002, Matsuda *et al*. 1999). Traditionally, AAFs are considered to be independent on wind fields, and hence arbitrary wind fields in wind tunnels have been used to identify them. As above discussed, if AAFs of bluff sections are inherently dependent on the oncoming wind properties, an issue arises as regards the applicability of the traditional method, since the wind fields used in wind tunnel may differ significantly from those at the bridge sites. If this dependence of AAFs is to be considered, wind fields used in wind tunnel need to resemble those in sites, and designers should always be cognizant of the possible influence when such resemblance cannot be satisfied.

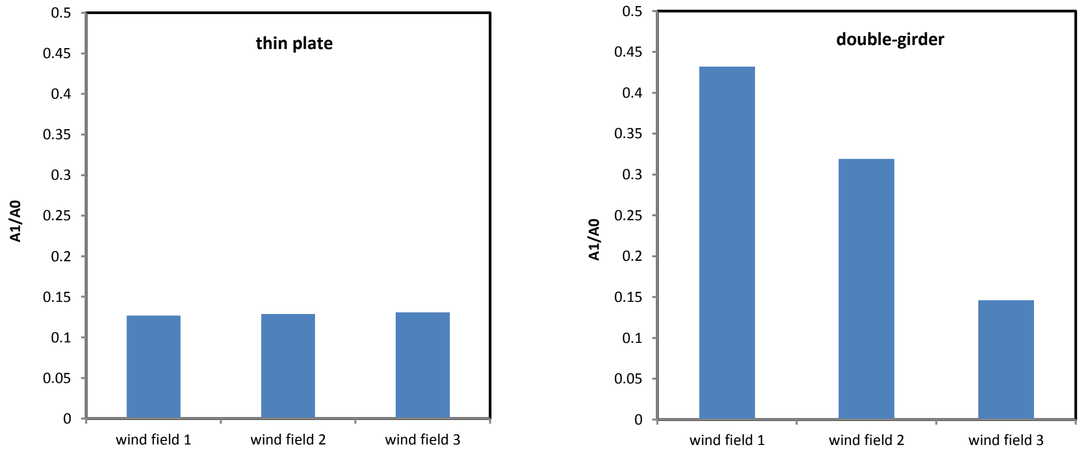

(a) thin plate (b) double-girder

Fig. 15 Ratios of the amplitude of lift to wind ($k = 0.8$)

4. Conclusions

In this paper, two AAF models that have been applied quite extensively in bridge aerodynamics are addressed. Both models adopt the methodology of deriving AAFs from known flutter derivatives; that is, in essence, determining the unsteady buffeting loads by the aeroelastic property. By assuming equivalence between the Wagner and the Küssner functions, the first model sets up directly the relation between AAFs and flutter derivatives. It is revealed this model is only applicable to very low reduced frequencies, which are much lower than predominant buffeting frequencies of long-span bridges immersed in fields of low-to-moderate wind speeds.

The second model introduces a relation between 'equivalent' Theodorsen circulation function and 'equivalent' Sears function, similar to that hold for thin airfoils. In so doing, an approach is also established to derive AAFs from flutter derivatives. However, a fundamental illogicality is revealed in this model either; that is, no appropriate 'equivalent' Bessel functions exists for the relation.

A viewpoint is put forward that AAFs of bluff bridge deck sections are inherently dependent on the coming wind properties, and this dependence is investigated with comparisons between a thin plate and a double-girder section. The results show that the AAFs of the bluff double-girder section exhibit obvious dependence on basic properties of oncoming wind fluctuations. In view of this, it is recommended that AAFs of bluff bridge deck sections be identified in wind fields possess similarity to those at bridge sites.

Acknowledgements

For the work described in this paper, the authors would like to give thanks to the financial support from the National Natural Science Foundation of China (Grant Number 51578233 and 51178182).

References

Caracoglia, L. (2008), "Influence of uncertainty in selected aerodynamic and structural parameters on the buffeting response of long-span bridges", *J. Wind Eng. Ind. Aerod.*, **96**, 327-344.

Caracoglia, L. and Jones, N.P. (2003), "Time domain vs. frequency domain characterization of aeroelastic forces for bridge deck sections", *J. Wind Eng. Ind. Aerod.*, **91**(3), 371-402.

Chen, X. and Kareem, A. (2001), "Nonlinear response analysis of long-span bridges under turbulent winds", *J. Wind Eng. Ind. Aerod.*, **89**(14-15), 1335-1350.

Chen, X., Matsumoto, M. and Kareem, A. (2000), "Time domain flutter and buffeting response analysis of bridges", *J. Eng. Mech. - ASCE*, **126**(1), 7-16.

Costa, C. (2007), "Aerodynamic admittance functions and buffeting forces for bridges via indicial functions", *J. Fluid Struct.*, **23**(3), 413-428.

Costa, C. and Borri, C. (2007), "Olivier Flamand, O, Grillaud G. Time-domain buffeting simulations for wind-bridge interaction", *J. Wind Eng. Ind. Aerod.*, **95**(9-11), 991-1006.

Davenport, A.G. (1962a), "The response of slender, line-like structures to a gusty wind", *Proceedings of Institution of Civil Engineers*, **23**, 389-408.

Davenport, A.G. (1962b), "Buffeting of a suspension bridge by storm winds", *J. Struct. Div. - ASCE*, **88**, 233-264.

Davidson, L. (2005), "Hybrid LES-RANS: Inlet boundary conditions", *Proceedings of the 3rd National Conference on Computational Mechanics*, Trondheim, Norway.

Diana, G., Bruni, S., Cigada, A. and Zappa, E. (2002), "Complex aerodynamic admittance function role in buffeting response of a bridge deck", *J. Wind Eng. Ind. Aerod.*, **90**(12-15), 2057-2072.

Garrick, I.E. (1938), "On some reciprocal relations in the theory of nonstationary flows", Langley: US Advisory Committee for Aeronautics, Langley.

Ge, Y.J. and Zhao, L. (2014), "Wind-excited stochastic vibration of long-span bridge considering wind field parameters during typhoon landfall", *Wind Struct.*, **19**(4), 421-441.

Ge, Y.J., Zou, X. J. and Yang, Y.X. (2009), "Aerodynamic stabilization of central stabilizers for box girder suspension bridges", *Wind Struct.*, **12**(4), 285-298.

Han, Y., Chen, Z.Q. and Hua, X.G. (2010), "New estimation methodology of six complex aerodynamic admittance functions", *Wind Struct.*, **13**(3), 293-307.

Hatanaka, A. and Tanaka, H. (2002), "New estimation method of aerodynamic admittance function", *J. Wind Eng. Ind. Aerod.*, **90**(12-15), 2073-2086.

Hatanaka, A. and Tanaka, H. (2008), "Aerodynamic admittance functions of rectangular cylinders", *J. Wind Eng. Ind. Aerod.*, **96**(6-7), 945-953.

Larose, G.L. and Mann, J. (1998), "Gust loading on streamlined bridge decks", *J. Fluid. Struct.*, **12**, 511-536.

Larose, G.L., Tanaka, H., Gimsing, N.J. and Dyrbye, C. (1998), "Direct measurements of buffeting wind forces on bridge decks", *J. Wind Eng. Ind. Aerod.*, **74-76**, 809-818.

Liepmann, H.W. (1952), "On the application of statistical concepts to the buffeting problem", *J. Aeronaut. Sci.*, **19**, 793-822.

Macdonald, J.H.G. (2003), "Evaluation of buffeting predictions of a cable-stayed bridge from full-scale measurements", *J. Wind Eng. Ind. Aerod.*, **91**, 1465-1483

Matsuda, K., Hikami, Y., Fujiwara, T. and Moriyama, A. (1999), "Aerodynamic admittance and the 'strip theroy' for horizontal buffeting forces on a bridge deck", *J. Wind Eng. Ind. Aerod.*, **83**, 337-346.

Minh, N.N., Miyata, T., Yamada, H. and Sanada, Y. (1999), "Numerical simulation of wind turbulence and buffeting analysis of long-span bridges", *J. Wind Eng. Ind. Aerod.*, **83**, 301-315.

Øiseth, O., Rönnquist, A. and Sigbjörnsson, R. (2011), "Time domain modeling of self-excited aerodynamic forces for cable-supported bridges: A comparative study", *Comput. Struct.*, **89**, 1306-1322.

Rasmussen, J.T., Hejlesen, M.M., Larsen, A. and Walther, J.H. (2010), "Discrete vortex method simulations of the aerodynamic admittance in bridge aerodynamics", *J. Wind Eng. Ind. Aerod.*, **98**, 754-766.

Scanlan, R.H. (2000), "Motion-related body force functions in two-dimensional low-speed flow", *J. Fluid.*

Struct., **14**, 49-63.
Scanlan, R.H. (2001), "Reexamination of sectional aerodynamic force functions for bridges", *J. Wind Eng. Ind. Aerod.*, **89**(14-15), 1257-1266.
Scanlan, R.H. and Jones, N.P. (1999), "A form of aerodynamic admittance for use in bridge aeroelastic analysis", *J. Fluid Struct.*, **13**(7-8), 1017-1027.
Scanlan, R.H. and Tomko, J.J. (1971), "Airfoil and bridge deck flutter derivatives", *J. Eng. Mech. Div.*, **97**(6), 1717-1737.
Sears, W.R. (1941), "Some aspects of non-stationary airfoil theory and its practical application", *J. Aeronaut. Sci.*, **8**(3), 104-108.
Tang, Y., Zheng, S.X. and Zhang, L.Q. (2015), "Numerical method for identifying the aerodynamic admittance of bridge deck", *Aca Aerod. Sinica*, **33**(5), 706-713. (in Chinese)
Theodorsen, T. (1935), "General theory of aerodynamic instability and the mechanism of flutter", Langley: US Advisory Committee for Aeronautics.
Tubino, F. (2005), "Relationships among aerodynamic admittance functions, flutter derivatives and static coefficients for long-span bridges", *J. Wind Eng. Ind. Aerod.*, **93**, 929-950.
Von Karman, T. and Sears, W.R. (1938), "Airfoil theory for non-uniform motion", *J. Aeronaut. Sci.*, **5**(10), 5-15.
Xu, Y.L., Sun, D.K., Ko, J.M. and Lin, J.H. (2000), "Fully coupled buffeting analysis of Tsing Ma suspension bridge", *J. Wind Eng. Ind. Aerod.*, **85**, 97-117
Zhang, W.M., Ge, Y.J. and Levitan, M.L. (2011), "Aerodynamic flutter analysis of a new suspension bridge with double main span", *Wind Struct.*, **14**(3), 187-208.
Zhang, Z.T., Ge, Y.J. and Chen, Z.Q. (2006), "A new aerodynamic method using in long-span bridge buffeting analysis", *Eng. Mech.*, **23**, 94-101. (in Chinese)
Zhang, Z.T., Ge, Y.J. and Zhang, W.F. (2013), "Superposability of unsteady aerodynamic loads on bridge deck sections", *J. Central South Univ. Technol.*, **20**, 3202-3215.
Zhu, L.D., Wang, M., Wang, D.L., Guo, Z.S. and Cao, F.C. (2007), "Flutter and buffeting performances of Third Nanjing Bridge over Yangtze River under yaw wind via aeroelastic model test", *J. Wind Eng. Ind. Aerod.*, **95**, 1579-1606.
Zhu, L.D., Xu, Y.L., Zhang, F. and Xiang, H.F. (2003), "Measurement of aerodynamic coefficients of tower components of Tsing Ma bridge under yaw winds", *Wind Struct.*, **6**(1), 53-70.
Zhu, Q. and Xu, Y.L. (2014), "Characteristics of distributed aerodynamic forces on a twin-box bridge deck", *J. Wind Eng. Ind. Aerod.*, **131**, 31-45.

AD